A Theoretical Study of the Catalytic Mechanism of Formate Dehydrogenase

R. Castillo, M. Oliva, S. Martí, and V. Moliner*

Departament de Química Física i Analítica, Universitat Jaume I, 12071 Castelló, Spain

Received: March 25, 2008; Revised Manuscript Received: May 13, 2008

A theoretical study of the hydride transfer between formate anion and nicotinamide adenine dinucleotide (NAD^+) catalyzed by the enzyme formate dehydrogenase (FDH) has been carried out by a combination of two hybrid quantum mechanics/molecular mechanics techniques: statistical simulation methods and internal energy minimizations. Free energy profiles, obtained for the reaction in the enzyme active site and in solution, allow obtaining a comparative analysis of the behavior of both condensed media. Moreover, calculations of the reaction in aqueous media can be used to probe the dramatic differences between reactants state in the enzyme active site and in solution. The results suggest that the enzyme compresses the substrate and the cofactor into a conformation close to the transition structure by means of favorable interactions with the amino acid residues of the active site, thus facilitating the relative orientation of donor and acceptor atoms to favor the hydride transfer. Moreover, a permanent field created by the protein reduces the work required to reach the transition state (TS) with a concomitant polarization of the cofactor that would favor the hydride transfer. In contrast, in water the TS is destabilized with respect to the reactant species because the polarity of the solute diminishes as the reaction proceeds, and consequently the reaction field, which is created as a response to the change in the solute polarity, is also decreased. Therefore protein structure is responsible of both effects; substrate preorganization and TS stabilization thus diminishing the activation barrier. Because of the electrostatic features of the catalyzed reaction, both media preferentially stabilize the ground-state, thus explaining the small rate constant enhancement of this enzyme, but FDH does so to a much lower extent than aqueous solution. Finally, a good agreement between experimental and theoretical kinetic isotope effects is found, thus giving some credit to our results.

Introduction

Formate dehydrogenase (FDH, EC 1.2.1.2) is a widely spread enzyme in nature that plays an important role, as it is one of the best enzymes for cofactor regeneration in the processes of chiral synthesis with nicotinamide adenine dinucleotide phosphate ($NAD(P)^+$)-dependent oxidoreductases.[1] It catalyzes oxidation of formate ion to carbon dioxide with concomitant reduction of NAD^+ to NADH (Scheme 1).

FDH has the biotechnological potential for use in organic acid synthesis as a catalyst in coenzyme regeneration systems for production of high added value pharmaceutical products.[2,3] The interest for FDH is also supported by the irreversibility of catalyzed reaction and the wide pH optimum of its activity.[4,5] FDH has been used for the determination of formic acid[6] and oxalic acid[7] in solution and in physiological fluids. Nevertheless, low operational stability and high production cost of native FDHs limit their application with commercial purposes, such as production of chiral compounds.[1] Site-directed mutagenesis studies on FDH have been also carried out with the aim to transform coenzyme specificity as well as to increase its turnover frequency factor or its thermal stability.[8] To this end, a detailed knowledge of the catalytic mechanism of FDH at the molecular level could provide guidelines for future protein engineering on this enzyme.

The enzyme consists of two identical subunits of 42 kDa each, each containing an independent active site. Although there are FDHs possessing metal ions or prosthetic groups in their active site, the one that is under study in this work does not apparently require them. Initial velocity and X-ray diffraction studies have

SCHEME 1: FDH Catalyzed Oxidation of Formate Ion to CO_2

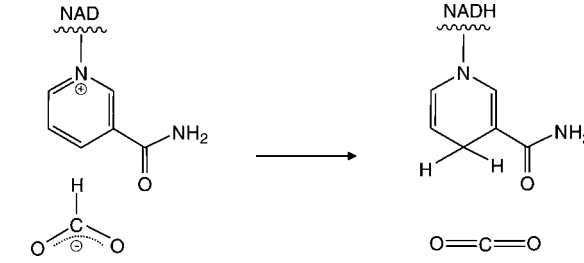

established an ordered kinetic mechanism in which NAD^+ binds the enzyme prior to formate binding. Then, a direct transfer of hydride ion from the substrate onto the C4 carbon atom of the nicotinamide ring of cofactor takes place in the ternary complex. This hydride transfer seems to be the sole rate limiting step in the catalytic mechanism of FDH.[9–11] The observed rate constant of 7.3 s^{-1},[12,13] shows that it is a relatively low efficient enzyme, compared to other NAD^+-dependent dehydrogenase, probably due to strong interactions between the substrate, in its ground state, and several residues of the active site.[14]

The fact that the chemical reaction was the rate-limiting step on FDH, together with some other advantages such as the absence of proton-release stages that exist in all dehydrogenase-catalyzed reactions, and considering that formate is structurally the simplest of dehydrogenase substrates, have allowed regarding this reaction as a model to be used in studies of the molecular mechanism. As pointed out by Tishkov and Popov in a recent review on protein engineering of FDH, the existence of

* Corresponding author.

10.1021/jp8025896 CCC: $40.75
Published on Web 07/23/2008

numerous FDH genes from various sources opens new horizons in improvement of enzyme properties with gene shuffling.[1]

In spite of the a priory simplicity of the chemical reaction catalyzed by FDH, the catalytic mechanism has been discussed arising from the analysis of two different locations of formate deduced from high resolution X-ray diffraction studies.[15] In any case, as this is a reaction in which charged reactants are transformed into neutral products, as pointed out by Popov et al., whatever the mode of formate binding, the mechanism of hydride transfer in FDH-catalyzed reactions appears to be governed by electrostatic effects.[15] Thus, it has been shown that most important residues for formate binding can be Arg284 and Asn146 or, alternatively, His332 and Asn146. On the other hand, Popov et al. suggested that the nicotinamide ring of the cofactor can interact by hydrogen bonds with Thr282, Asp308, Ser334, and Gly335.[15] It has been proposed that these residues can stabilize the initially positively charged ring, enhancing the electrophilic properties of the C4 atom by twisting the carboxamide group with respect to the pyridine plane and thus perturbating the ground state.[15] Li and Goldstein showed that coplanar trans conformation was the most stable conformation in gas phase, but interactions with some aminoacids can force its conformation in the active site to a energetically less preferred structure, by polarizing the pyridine ring and thus creating a partial positive charge on the hydride acceptor C4 carbon atom.[15,16]

These findings are related with one of the most important and discussed questions regarding NAD^+-dependent dehydrogenases, which concerns the conformation of the pyridine ring in the transition state (TS).[17] Several theoretical studies support the idea that ring puckering can reduce the activation barrier.[18–26] Nowadays, the small secondary ^{15}N kinetic isotope effects (KIEs) measured at the N1 position of 3-acetylpyridine adenine dinucleotide on the reaction catalyzed by FDH, close to unity, and gas-phase *ab initio* calculations by Tapia et al.[27] and Bruice et al.[14] suggest that N1 does not undergo an appreciable decrease in bond order during hydride transfer.[28] Thus, the nitrogen center of the pyridine ring would remain essentially planar during the reaction,[28] in accord with gas-phase calculations[18,20–22,29–35] but in contrast with the deformation mechanism previously postulated.

Other KIEs, such as ^{13}C at the C4 position and primary deuterium KIEs, have been measured for yeast FDH, rendering values of 1.043 and 2.8, respectively.[10] In this work, Blanchard and Cleland presume that the oxygens of formate were held by the enzyme while hydride transfers and the carbon of formate moved in opposite directions. The measured intrinsic deuterium isotope effect was relatively low compared with previous reported values for other dehydrogenases. These values, considering the traditional idea that primary KIEs are largest when TS is at the midpoint of the advance between reactants and products, make them suggest that data probably resulted from a late TS and demonstrated that an intrinsic deuterium isotope effect arising from deuteroformate was fully expressed on the kinetic parameter *V/K*. This magnitude measures substrate capture, a conclusion that was supported by the relative large ^{13}C effect of 1.043 and the behavior of azide as a TS analogue. Azide, with its full positive charge at N2, full negative charges at N1 and N3, and linear structure, fulfills all requirements for the predicted TS.[10] Blanchard and Cleland also measured ^2H-KIE values of 4.4 for thio-NAD, 6.9 for acetylpyridine-NAD and 3.8 for pyridinecarboxaldehyde-NAD, which would represent earlier TSs.[10] Moreover, LeReau et al.[36] show a deuterium KIE at C4 of the nicotinamide ring upon binding of NAD to lactate dehydrogenase (LDH) of ca. 10%, which argues for the development of carbonium ion character at this carbon atom. As pointed out by Rotsberg and Cleland,[28] if this character appeared at C4 without changing the bond order to N1, the enzyme must be stabilizing a dipolar form such as the one presented in Scheme 2.

SCHEME 2: Dipolar Form of the Nicotinamide Ring of NAD^+ As Suggested by Rotsberg and Cleland[28]

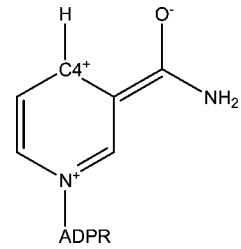

The formation of this complex would be in agreement with site-directed mutagenesis studies on FDH carried out by Popov et al.,[37] showing that the His332−Gln313 pair is essential for enzyme activity. Although the role of histidine is discussed, as it was shown that protonation state of His332 is not critical for catalysis but vital for substrate binding, it seems to provide favorable electrostatic interaction. More recent site-directed mutagenesis studies by Popov et al.[38] have confirmed previous conclusions derived from X-ray diffraction structures,[15] that Arg284 is directly involved in substrate binding and supporting the catalytic conformation of the enzyme active site. An additional role has been ascribed to this essential residue by participating in catalysis through polarizing of the carbonyl group of the substrate, a role similar to the one assigned to Arg109 in L-specific LDH.[39] Classical molecular dynamics (MD) simulations performed on the active site of FDH from *Pseudomonas* sp. 101 by Bruice et al.[40] showed that formate is placed by a persistent bifurcated hydrogen bond between one formate oxygen and the guanido hydrogens of Arg284, and a single hydrogen bond from the other oxygen of formate and Asn146 and Ile122. The simulations also suggested that His332 plays a role in both binding of formate and the generation of near-attack conformations (NAC). The conclusions Bruice et al. derived from analysis of the electrostatic interactions at the active site of the enzyme with substrate and TS[41] were that changes were not consistent with the hypothesis of preferential stabilization of the TS over the ground state.[40]

The present paper is focused on the application of techniques provided by computational chemistry applied to understand the physical basis of the rate enhancement of the chemical reaction catalyzed by FDH. The theoretical results will be compared with previously published kinetic and structural data, allowing validating, to some extent, our procedures and predictions.

Computational Details

The initial coordinates for the enzyme calculations were taken from the X-ray crystal structure of the *Pseudomonas* sp. (Protein Data Bank: 2NAD)[15] complexed with azide inhibitor in the formate binding site. Once the azide molecule was replaced by the product of the FDH catalyzing reaction, CO_2, hydrogen atoms were incorporated into the structure to a state complementary to pH 7, using the DYNAMO program.[42,43] Then, the system, centered on C4 of the cofactor (see Scheme 3) of subunit B, was placed in the mass center of a cavity deleted from a pre-relaxed box of water molecules ($80 \times 80 \times 80$ Å^3). All the water molecules with an oxygen atom lying within 2.8 Å of any heavy atom were removed. Because of the size of the

SCHEME 3: Details of the FDH Active Site[a]

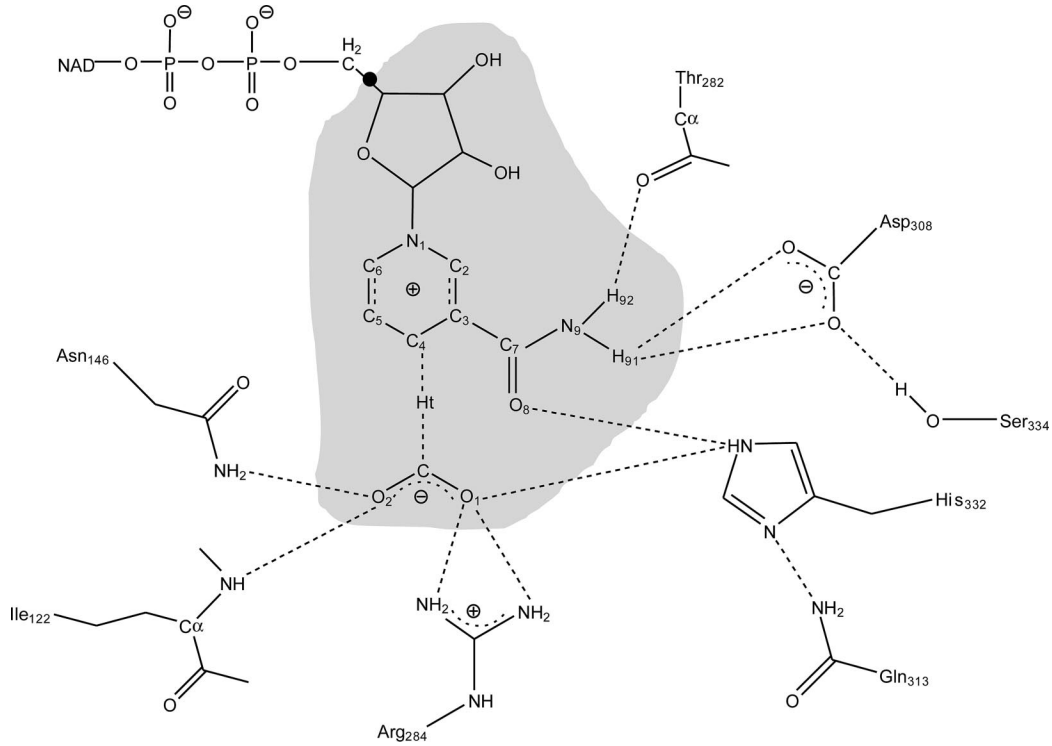

[a] Shaded region corresponds to the QM subset of atoms, while the link atom is indicated as •.

system, all the residues further than 38 Å from the C4 of the cofactor were removed, and those further than 18 Å were kept frozen (20314 atoms from a total of 23919 atoms).

The entire chemical system was divided into a quantum mechanics (QM) region, comprising the product CO_2 together with the nicotinamide and the ribose rings of the NADH cofactor (33 atoms), and a molecular mechanics (MM) region, which includes the rest of the system (the rest of the cofactor, the protein model and crystallization, plus solvation water molecules). The AM1[44] semiempirical Hamiltonian was selected to describe the QM region, and the OPLS-AA[45] and TIP3P[46] force fields were chosen for the MM region. The link atom method[47,48] was used to treat the covalent bond crossing the boundary between the QM and the MM regions, in order to satisfy the valence of the QM fragments (see Scheme 3). To treat the nonbonding interactions, a switch function with a cutoff distance in the range of 8−12 Å was used.

Hybrid QM/MM potential energy surface (PES) explorations (from products to reactants) and transition structure location and characterization were carried out, guided by means of the micro−macro iterations scheme.[49] In this method, the system is divided into two parts, the core or control space and the environment or complementary space, being the Hessian matrix explicitly calculated only for those atoms belonging to the core. Once this partitioning has been done, the saddle point location is carried out in the degrees of freedom of the core, under a fully relaxed environment. Thus, before each gradient or Hessian guided step for the core, the degrees of freedom of the environment are optimized in order to maintain an approximately zero gradient and to minimize the potential energy. In our case, the core region contains all the QM atoms.

The free energy profile, in terms of potential of mean force (PMF), was calculated using the weighted histogram analysis method (WHAM) combined with the umbrella sampling (US) approach,[50,51] as implemented in DYNAMO. The starting geometry for these calculations was the saddle-point structure previously located on the PES, while the distinguished reaction coordinate was taken as the antisymmetric combination of the distances describing the breaking and forming bonds, i.e., $dCH_t - dH_tC4$ (see Scheme 3). This variable was confirmed to be the most representative coordinate changing along the reaction path, and was this the natural choice for determining the PMF. The procedure for the PMF calculation was straightforward and required a series of hybrid QM/MM MD simulations in which the reaction coordinate variables were restrained about particular values. The values of the variables sampled during the simulations were then pieced together to construct a full distribution function from which the PMF was obtained. A total of 65 simulations were performed at different values of the reaction coordinate, with an umbrella force constant of 2000 $kJ \cdot mol^{-1} \cdot Å^{-2}$ for each particular value. On each window, 2 ps of relaxation Langevin MD followed by 10 ps of production were computed. The time step for integrating the equations of motion was chosen as 0.5 fs because of the nature of the chemical step involving a hydrogen transfer. The Verlet algorithm was used to update the velocities, and the bath temperature was 300 K.

Afterward, QM/MM MD simulations were performed for the ground-state and TS to analyze the main geometrical parameters and evaluate the interaction energy between the reacting fragment and the protein. For this purpose, a Langevin bath with a coupling temperature of 300 K was employed throughout this work, using the canonical thermodynamic ensemble (NVT). A total run of 1000 ps for each simulation was made with an integration step size of 0.5 fs. During the MD trajectory for the TS simulation, the reaction coordinate variable was restrained to the value corresponding to that on the maximum of the PMF, with a force constant of 10000 $kJ \cdot mol^{-1} \cdot Å^{-2}$. From this last trajectory, 10 structures were selected as starting points to locate and refine first-order saddle points on the PES (that define TS

structures) by means of the micro−macro iterations scheme stated above. Subsequent reaction coordinate paths (ESRP or ES1RP)[52] were traced down toward the corresponding minima (reactants or products), followed by a global optimization procedure. Each step of the reaction path was obtained applying a control/complementary space technique, thus the gradient vector of the QM atoms was computed after complete relaxation of the MM atoms. The difference between this and the true intrinsic reaction coordinate (IRC) path, which was traced down from the saddle point to the corresponding minima using the full gradient vector, was trivial, since the core was selected so that the contributions of the atoms outside the core was almost negligible. Also, it was essential to use a small step size in the IRC computation, in order to allow the environment to relax at every single step and to prevent the algorithm from halting falsely or from loosing the right direction.

The rigid-rotor/harmonic-oscillator approximation was used with the CAMVIB/CAMISO programs[53,54] to calculate the KIEs at 300 K. In order to obtain averaged values, the previous 10 reactants/transition structure pairs were selected. In common with other vibrational properties such as IR spectroscopic frequencies, isotope effects are local properties[55] in the sense that they are determined by the immediate environment of the center of isotopic substitution; this local environment extends only by one or two bond distances ("cutoff rule"). This justifies the fact that the ratios of partition functions were calculated not for the whole enzyme, but only for a subset of the full system. In this sense, KIEs were calculated by using the core subset of atoms (equivalent to the QM region) to compute the Hessian matrix in the presence of the environment effect. All force constants and vibrational frequencies were used without scaling in these calculations, estimating tunneling effects by means of the Bell equation.[56]

In order to overcome the limitations of the selected AM1 semiempirical Hamiltonian, an MP2/MM method was used with the aim of obtaining representative potential energy results. For this purpose we have made use of two calculation protocols. Initially, the transition structure was located and characterized using an uncoupled *ab initio* HF(6-31G**)/MM scheme. In this approach we profit from the control space/complementary space optimization techniques by changing the way the coupling between QM and MM regions is calculated. During the control space (which usually fits with the QM atoms) optimization, the classical atoms are introduced in the selected electronic Hamiltonian as a charge distribution, thus interacting with the molecular orbital. On the other hand, during the complementary space (MM atoms) optimization, the QM atoms are kept frozen, and the interaction between both subsystems is described by a pure classical Coulomb expression, in which the QM atoms are represented by punctual electrostatic fitted charges:

$$E_{\text{control}} = E_{\text{MM}} + \langle \Psi | \hat{H}^{\circ}_{\text{ab initio}} | \Psi \rangle + \left\langle \Psi \left| \frac{Q_{\text{MM}}}{r_{\text{QM/MM}}} \right| \Psi \right\rangle + E^{\text{Lennard-Jones}}_{\text{QM/MM}} \quad (1)$$

$$E_{\text{complementary}} = E_{\text{MM}} + \sum \frac{q^{\text{FIT}}_{\text{QM}} Q_{\text{MM}}}{r_{\text{QM/MM}}} + E^{\text{Lennard-Jones}}_{\text{QM/MM}} \quad (2)$$

where E_{MM} accounts for the energy of the force field (protein plus solvent molecules), Ψ is the QM wave function polarized by the presence of the external electrostatic field due to the classical environment, and $\hat{H}^{\circ}_{\text{ab initio}}$ is the selected gas phase Hamiltonian operator. The advantage of this scheme relies on the large number of optimization cycles that are usually needed during the environment relaxation (complementary space). The selected algorithm to evaluate the electrostatic fit for the QM atomic charges is the ChelpG method,[57] which makes use of the polarized wave function. These charges are later introduced in the classical Coulombic electrostatic potential function between QM and MM regions. Equations 1 and 2 can be expressed in terms of the gradient vector or the Hessian matrix, in order to be applied in common optimization algorithms. In our work, the Hessian matrix computed just for the control space was only recalculated every 10 optimization steps, being updated by means of the Bofill algorithm[58] in the rest of the steps.

The reactant structure was localized from the optimization of the last point of the reaction path traced down from the previously located transition structure, applying the same methodology and algorithms. Full MP2(6-31G**)/MM single-point calculations were performed in each of the optimized structures in order to provide a better estimate of the activation energy.

To rationalize the catalytic effect of the enzyme, a comparative study of the reaction in water was performed. This comparative analysis will be also used to understand the particular behavior of the enzyme active site in the reactant state. The coordinates of the quantum atoms from the TS located and characterized in the protein environment were the starting point to build up the aqueous solution model. These fragments, centered on C4 of the cofactor (see Scheme 3), were placed in the mass center of a cavity deleted from a prerelaxed cubic box of water molecules (55.8 Å side). All the water molecules with an oxygen atom lying within 2.8 Å of any heavy atom were removed. The QM region is the same as the one in the enzyme and it was also described using the AM1 semiempirical Hamiltonian. The MM region is composed by 5509 water molecules described by means of the TIP3P force field. To treat the nonbonding interactions, periodic boundary conditions were applied, using a switch function with a cutoff distance in the range of 8−12 Å.

The PMF in water was calculated using the same reaction coordinate, force constant, time step, temperature, relaxation, and production time as in the enzyme. However, because of the high mobility of the formate fragment, the angle $C(CO_2)-H_t-C4(NAD)$ was restrained with a force constant of 8 $kJ \cdot mol^{-1} \cdot degree^{-2}$.

The contribution of this additional restrain to the calculated activation free energy has been removed by means of thermodynamic integration methods. For this purpose, a series of hybrid QM/MM MD simulations (using the same ensemble, coupling temperature and integration algorithm) have been run for both reactant complex and transition structure, at different values of a parameter λ coupled to the restrain energy:

$$U(R,\lambda) = U(R) + \lambda \frac{1}{2} K_{\text{Umb}} (\theta - \theta^{\circ})^2 \qquad \lambda = 0, \ldots, 1 \quad (3)$$

$$\Delta F_{\text{restraint}} \approx -\frac{1}{N_\lambda} \sum_{N_\lambda} \frac{K_{\text{Umb}}}{2 n_k} \sum_{n_k} (\theta - \theta^{\circ})^2 \quad (4)$$

where $U(R)$ is the QM/MM potential energy function, and K_{Umb} and θ° are the aforementioned reference angle and force constant of the restrain, respectively.

Also, in order to validate this method, a free energy perturbation (FEP) study of the chemical reaction step was studied in aqueous solution. Thus, a full relaxed reaction path was traced down starting from the previously localized and characterized TS. Then for each of the selected points along the reaction path, a series of hybrid QM/MM MD simulations

were carried out in which the QM atoms were kept frozen. Thus, the activation free energy for the process was obtained from the approximated forward expression:

$$\Delta F_{i\rightarrow j} \approx \Delta E^{\mathrm{QM}}_{\mathrm{gas\text{-}phase},i\rightarrow j} - \frac{1}{\beta} \ln \langle e^{-\beta \Delta E^{\mathrm{QM/MM}}_{\mathrm{int},i\rightarrow j}} \rangle_i \qquad (5)$$

where $\Delta E^{\mathrm{QM}}_{\mathrm{gas\text{-}phase},i\rightarrow j}$ accounts for the QM energy difference in the gas phase of the consecutive points along the reaction paths *i* and *j*, and $\Delta E^{\mathrm{QM/MM}}_{\mathrm{int},i\rightarrow j}$ is the corresponding difference of interaction energy between the QM atoms (configurations *i* and *j*) and the environment of the dynamical trajectory *i*. The same scheme can be applied to the backward direction along the reaction path, providing in this way an estimate of the error of the calculation.

Finally, as done in the enzyme, 800 ps QM/MM MD simulations were performed restraining the reaction coordinate with a force constant of 10 000 kJ·mol^{-1}·Å^{-2}, first, at the value corresponding to that on the maximum of the free energy profile (TS), and second to a value equal to the one obtained in the Michaelis complex located in the enzyme active site (MC-like).

Results and Discussion

The Free Energy Profile. Theoretical estimation of an enzyme activity can be done by means of the free energy barrier of the rate-limiting step and, if possible, comparison with the equivalent reaction in solution. Nevertheless, from a computational point of view, calculation of the free-energy barrier of a bimolecular reaction, which is the kind of reaction catalyzed by FDH, in water would require evaluation of the free-energy change for bringing the reactants together and of orienting them properly, followed by the study of the chemical reaction itself (the breaking and forming of bonds). As enzymes present the ability of binding substrate(s) with an appropriate conformation capable of progressing to the TS (the Michaelis complex (MC)), the formation of a reactant complex in solution could be defined as species with an MC-like geometry (MC-like structure). From a phenomenological point of view, in the case of a reaction where charged reactants are transformed into neutral products, this process involves the formation of an ion-pair from isolated, fully solvated, cations and anions. This quantity involves a balance of opposing contributions: on one hand there are unfavorable losses of translational and rotational entropy and of solvation enthalpy, but on the other hand there are favorable gains in entropy of solvation and cation−anion interaction enthalpy that accompany ion-pair formation. In practice, a PMF computed for the association of two solute molecules (or dissociation of their complex) in aqueous solution should provide a correct estimate for the free energy of association, provided that certain conditions are met. Thus, restraints had to be applied to the solute until arriving at completely solvated species; otherwise, full relaxation of the system in solution could render a complex not related to the studied reaction pathway. For instance, in the case of the reaction catalyzed by FDH, an ester adduct by nucleophilic addition, instead of 1,4-dihydropiridine via hydride transfer, would be obtained, as previously observed by Bruice et al. from gas-phase and model systems calculations by continuum solvation methods.[14] These features are in accordance with the fact that no experimental data is available for this reaction in water. Accordingly, in the present paper we are comparing the free-energy barrier from MC to TS in the enzyme with the free energy change from an MC-like contact ion pair structure (with a reaction coordinate equivalent to the one observed for the MC in the enzyme, as explained in the Computational Details section) to the TS in solution.

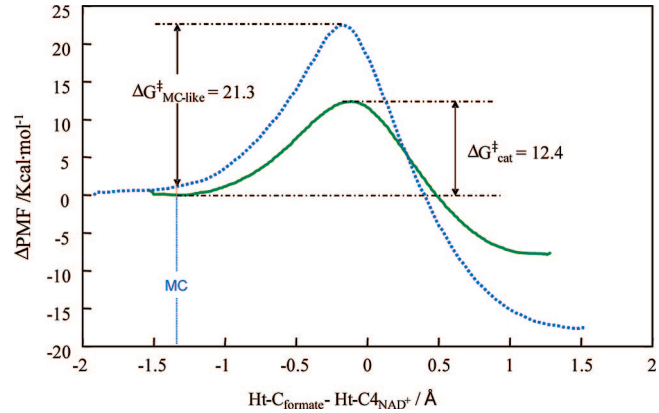

Figure 1. PMF of oxidation of formate anion to carbon dioxide, catalyzed by FDH (green solid line) and in aqueous solution (blue dashed line).

The PMF for the oxidation of formate anion to carbon dioxide catalyzed by FDH, together with the reference model reaction in solution, is depicted in Figure 1. It is worth mentioning that, as previously discussed, the MC-like state is not a real minimum in the aqueous solution free energy surface. Moreover, a note of caution has to be introduced at this point, as the reaction under study implies that the transfer of a light particle and quantum tunneling can take place. Nevertheless, tunneling usually has a minor acceleration effect compared to the corresponding uncatalyzed reaction in water. It may indeed occur in enzyme reactions, but it does not dramatically contribute to enzymatic catalysis since similar tunneling effects exist in the solution reaction.[59] Thus, and although other groups consider tunneling an alternate way to look at the catalysisis rather than a correction,[59] keeping in mind that we are comparing the chemical reaction in both media, this possible source of error must be relatively small in the reaction under study and would not invalidate our conclusions. Anyway, this is an open question and more theoretical and experimental studies have to be devoted to this controversal subject in order to elucidate the impact of tunneling contribution to enzyme catalysis.

As observed in Figure 1, the free energy barrier of the reaction in the enzyme, 12.4 kcal·mol^{-1}, is much smaller than the corresponding one in solution, 21.3 kcal·mol^{-1}, demonstrating the catalytic activity of the enzyme, $\Delta\Delta G^{\ddagger} = 8.9$ kcal·mol^{-1}. Nevertheless, it must be kept in mind that the MC-like state defined in aqueous solution is not a minimum, so the 8.9 difference has to be considered as a lower limit of the free energy barrier difference between the two media. As explained in the previous section, the free energy profile in water has been also obtained by means of FEP methods rendering almost virtually the same activation free energy, thus providing a consistent result (see Supporting Information). The experimental value of the free energy barrier, estimated from the rate constant reported in the literature for *Pseudomonas* sp. 101 FDH catalyzed reaction,[12,13] is 16.6 kcal·mol^{-1}, which is in good agreement keeping in mind that the reported experimental data is not for single-step but for a complex rate constant that is composed of multiple "microscopic rate constants". It means that experimental measurement has to be considered the upper limit of our single-step theoretical prediction. Nevertheless, in an attempt to check possible errors coming from the AM1 semiempirical Hamiltonian employed in our simulations, single-

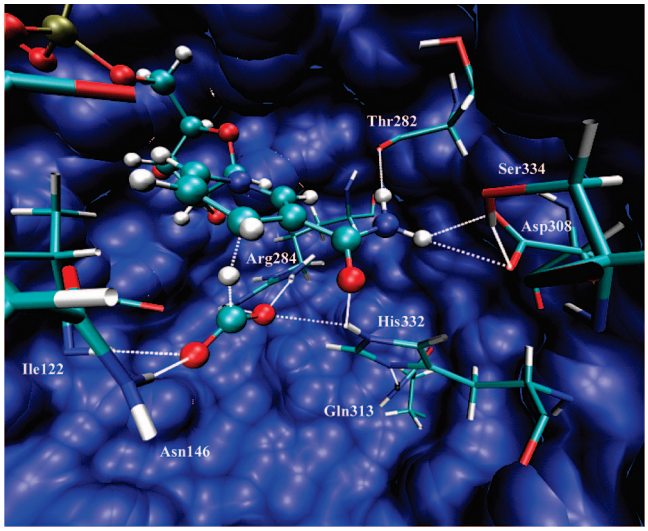

Figure 2. Representative snapshoot of the active site of the enzyme in the TS conformation. Substrate and cofactor are displayed as balls and sticks, while key residues of the enzyme active site are in liquorice.

point MP2/MM calculations have been performed with previously optimized HF/MM geometries of the reactants and TS. The activation energy was 12.4 kcal·mol^{-1}, which is the same result as the one obtained at the semiempirical level of theory and gives some credit to our calculations.

As described in the Computational Details section, once the PMFs were obtained, long hybrid QM/MM MD simulations were carried out using the US approach to restrain the system close to the particular value of the reaction coordinate at the corresponding state. These calculations allow estimating the solvent−solute or enzyme−substrate interaction energy, and, as explained elsewhere,[60] the first 300 ps of the QM/MM MD simulations are discarded. The solvent−solute and enzyme−substrate interaction energy contributions to the barrier have a value of 50.0 and 77.5 kcal/mol in the enzyme and water, respectively. Keeping in mind that the reaction involves annihilation of charges in going from reactants to products, a polar medium such as water or charged amino acids of the protein interact much strongly with the reactants than with the TS; the solute−solvent and substrate−protein interaction energies are greater for the reactants than for the TS. Nevertheless, our results clearly show how, in comparative terms, protein interacts much better than the water molecules of the aqueous solution with the TS. Consequently, the catalytic character of the enzyme, in comparison with the reaction in solution, comes from the lower unfavorable enzyme−substrate interaction energy in going from MC to TS.

Substrate Binding Site at the Ground-State and Transition State. Figure 2 displays a representative snapshot of the active site of the enzyme in its TS configuration, while key averaged values of geometrical parameters of the substrate and cofactor, as well as interaction distances with amino acids of the protein, are listed in Table 1.

Information reported in Table 1 has been organized into two blocks; a set of structural information related to the QM region (substrate and nicotinamide ring of the NAD$^+$), and several distances corresponding to hydrogen bond interaction participating residues of the active site. Also, information of the aqueous solution calculations is presented for comparative purposes. The first geometrical feature to comment on is the fact that transferred hydride is almost in between the donor and acceptor carbon atoms in the TS, in a slighter more advanced stage in the enzyme than in water (−0.172 and −0.111 Å in water and in the enzyme environment, respectively).

With regard to the angle defined by the donor atom, the hydride and the acceptor atom, C(CO_2)−H_t−C4(NAD), both TSs also present similar values, while large deviations are obtained at the MC and MC-like complexes (104.06 and 139.53, respectively). We must keep in mind that MC-like in solution was obtained by fixing the reaction coordinate, which could bias the geometrical analysis.

Another interesting observation is the relative orientation of the amide group of the nicotinamide ring, monitored by the O8−C7−C3−C4 dihedral angle. Thus, the large value of the standard deviation of this dihedral angle in solution (ca. 90°) reflects the large fluctuation of the amide group. In contrast, protein keeps the geometry of amide group fixed at ca. 20° from MC to TS, with a very small deviation (ca. 8°) that shows a robustness of the orientation imposed by the enzyme active site. This result is in agreement with Popov et al. studies on the *a priori* unexpected structure of the amide group from X-ray diffraction studies on the FDH−azide inhibitor complex. The protein effect on the amide group orientation is particularly interesting, as is not stabilizing the most stable conformation; the *trans* conformer is the most stable one by ca. 2 kcal·mol^{-1} at gas phase AM1 level of theory. This behavior was already observed by Bruice et al., although from gas-phase[14] and classical MD simulations carried out in the enzyme.[40]

The electrostatic consequences of this observed deformation of the cofactor imposed by the protein will be discussed in next subsection, but it is interesting to note the relationship with the carbonyl group of the amide group. Thus, the C7−O8 double bond is slightly elongated when going from reactants to TS, a variation coupled with a decrease in the C3−C7 distance. Even though differences are really small, they are larger in the enzyme than in water, thus whatever consequence it had, they will be larger in the enzyme environment, as discussed later on. Moreover, its elongation can be assisted by the interaction with His332. A stronger interaction between His332 and O8 in TS than in the MC would be in accordance with this interatomic distance change (see Table 1). These results are in accordance with conclusions derived by Rotsberg and Cleland[28] and with the gas-phase calculations of Bruice et al.[14]

Apart from the interactions with His332, another conclusion derived from the analysis of the rest of the distances corresponding to hydrogen bond interactions with residues of the active site is the fact that the pattern of interactions remains as a robust feature along the reaction profile. From an entropic point of view, these interactions are playing an important role by anchoring the formate ion in the MC and also preventing side-reactions between formate and NAD$^+$. In fact, hydrogen bond interactions between formate ion and Arg284, Ile122, Asn146, and His332 keep the substrate in the proper orientation to transfer the hydride to the cofactor, while those between the formamide moiety and Thr282, Asp308, Ser334, and His332 prevent possible rotations of the group and formation of an ester adduct.

A more exhaustive analysis of the evolution of these mentioned interactions during the hydride transfer reveals very interesting features. First, the distances defined between the oxygen atoms of formiate and Arg284 increases from reactants to TS, which is related to a less polarized carbon−oxygen bond and, consequently, a less negative charge on O atoms of the substrate. These movements favor the stabilization of TS, which can be compared to the role of Arg109 in LDH.[39,61–63] In this

TABLE 1: Selected Interatomic Distances (in Å) and Angles (in Degrees) Obtained at the MC-like State and TS for Aqueous Solution, and MC and TS in the Enzyme[a]

	aqueous solution		enzyme	
	MC-like	TS	MC	TS
C4(NAD)-C(CO_2)	3.365 ± 0.175	2.712 ± 0.075	3.083 ± 0.171	2.662 ± 0.064
Ht-C4(NAD)	2.458 ± 0.033	1.468 ± 0.034	2.640 ± 0.332	1.415 ± 0.032
Ht-C(CO_2)	1.131 ± 0.029	1.296 ± 0.033	1.128 ± 0.030	1.304 ± 0.031
C(CO_2)-Ht-C4(NAD)	139.53 ± 17.91	160.20 ± 9.99	104.06 ± 20.29	157.80 ± 7.92
O8−C7−C3−C4	153.26 ± 80.26	175.56 ± 99.36	24.74 ± 8.56	20.56 ± 7.49
O8−C7	1.257 ± 0.018	1.260 ± 0.018	1.260 ± 0.017	1.266 ± 0.018
C7−C3	1.500 ± 0.026	1.490 ± 0.026	1.504 ± 0.026	1.491 ± 0.026
C2−C3−C5-C4	179.82 ± 5.55	171.49 ± 6.41	175.80 ± 5.22	167.10 ± 5.07
C6−C5−C3-C2	−0.14 ± 4.30	−0.18 ± 4.35	0.65 ± 4.05	0.93 ± 4.03
C5−C6−C2-N1	179.69 ± 5.55	177.02 ± 6.31	177.36 ± 5.27	173.79 ± 5.81
O2(CO_2)-HD21 Asn146			1.990 ± 0.165	1.978 ± 0.151
O2(CO_2)-H Ile122			1.948 ± 0.159	2.034 ± 0.158
O1(CO_2)-HH22 Arg284			2.140 ± 0.269	2.461 ± 0.293
O1(CO_2)-HH12 Arg284			1.924 ± 0.169	2.048 ± 0.179
O2(CO_2)-HH22 Arg284			3.403 ± 0.216	3.770 ± 0.207
O2(CO_2)-HH12 Arg284			4.097 ± 0.189	4.270 ± 0.189
O1(CO_2)-HE2 His332			2.290 ± 0.258	2.381 ± 0.250
O8(NAD)-HE2 His332			2.340 ± 0.247	2.165 ± 0.212
H92(NAD)-O Thr282			1.884 ± 0.151	1.898 ± 0.146
H91(NAD)-OD1 Asp308			2.342 ± 0.238	2.361 ± 0.231
H91(NAD)-OD2 Asp308			2.431 ± 0.296	2.412 ± 0.295
H91(NAD)-OG Ser334			2.764 ± 0.226	2.721 ± 0.217
HG Ser334-OD2 Asp308			1.730 ± 0.144	1.751 ± 0.155
ND1His332-HE21 Gln313			3.427 ± 0.163	3.442 ± 0.159
ND1His332-HE22 Gln313			1.865 ± 0.125	1.862 ± 0.120

[a] Averaged values together with the root-mean-square (rms) deviations come from AM1/MM MD simulations.

regard, Taguchi and co-workers performed kinetic studies on catalytic reactions of D-LDH and FDH, both wild-type and mutant, indicating different roles of arginine residues in the catalytic reactions: stabilization of substrate binding and promotion of hydride transfer, respectively.[64] FDH structurally resembles D-LDH (EC 1.1.1.28), despite having less than 20% sequence similarity. D-LDH is an evolutionally unrelated enzyme[65–67] of L-LDH but catalyzes essentially the same reaction with only the chirality of the products differing.[68] The reaction catalyzed by the two LDH enzymes (reduction of pyruvate into lactate) implies a hydride transfer from NADH to the substrate and a proton transfer from an aminoacid of the protein backbone, His296 and His195 for D and L-LDH, respectively. FDH possesses highly conserved residues His332 and Arg284 (amino acid numbering is according to that for *Pseudomonas* sp. 101 FDH[17]) at the positions corresponding to His296 and Arg235 of D-LDH, respectively.[17] In our theoretical simulations of the LDH enzymatic reaction,[61–63] the distance between the carbonyl oxygen atom of pyruvate and Arg109 decreases when going from MC to TS, thus creating also a stabilization of TS by polarizing the carbonyl bond. In both enzymes, the charge on the acceptor carbon atom (C4 of NAD^+ in FDH and C1 of pyruvate in LDH) becomes more positive, thus facilitating the hydride transfer. Focusing on the interactions between the protein and the cofactor, the behavior of the binary His332−Gln313 is especially interesting. It seems that the almost invariant interaction between these residues facilitates the interaction of the former with the carbonyl group of the formamide moiety of the nicotinamide ring by maintaining the protonation state of His332, required for substrate binding. This is in agreement with site-directed mutagenesis by Popov et al.[37] showing that His332Phe mutation leads to a complete loss of enzyme activity, while Gln313Glu mutation shifts the pK of the group controlling formate binding from less than 5.5 in wild-type enzyme to 7.6.[37] In fact, our simulations shows how the His332−O8 distance decreases from MC to TS (see Table 1), provoking the polarization of the carbonyl bond and, as a consequence, an increase of the negative charge on the O8 atom and a decrease on the C4 atom (more positive). Again, this can be interpreted as a stabilization of the TS. Moreover, as recently demonstrated by Bandaria et al. from infrared photon echo spectroscopy measurements of FDH in ternary complex with azide, fast protein−ligand interaction dynamics may be functionally important.[69] In this sense, further theoretical studies demonstrating this dynamic role of the enzyme or the participation of these residues in the reaction coordinate are in progress.

Electrostatic Effects. The study of the electrostatic effects has been carried out in two steps: first, by computing the charge evolution on the key atoms of substrate and cofactor under the effect of the aqueous solution or the protein, and second, by more global effects, which are the electric field and the electrostatic potential created by the environment on the hydride position along the reaction profile. Figure 3 displays the population analysis on key atoms involved in the chemical reaction along the reaction profile, in the gas phase, in water, and in the enzyme.

As observed in Figure 3a, the evolution of charge on the donor atom, more positive in products than in reactants state, is reasonable if we keep in mind that a hydride transfer is taking place from this carbon atom to the cofactor, i.e., reactants represent a negative ion species, and the product is a carbon dioxide molecule. Nevertheless, it is important to point out that the value observed in the TS in water (ca. 0.46) is almost the one reached at the products (ca. 0.45), while the charge evolution in the enzyme is smoother (ca. 0.44 and 0.51 au in TS and products, respectively). Perhaps more surprising is the charges evolution on the acceptor atom, C4, and the hydride atom, H_t. In the former (Figure 3b), the value observed in the TS is a maximum and positive, while the analysis of the hydride reveals that its charge on the TS is an absolute minimum (Figure 3c).

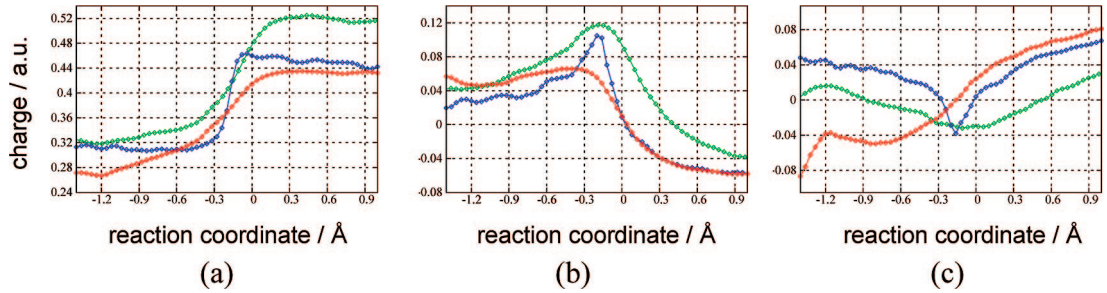

Figure 3. Averaged population analysis evolution (in au) on key atoms; (a) $C_{formiate}$, (b) $C4_{NAD^+}$ and (c) H_t along the reaction profile in the enzyme (green line), in solution (blue line), and in the gas phase (red line). Gas-phase population analysis was done with the structures of the substrate and the nicotinamide ring of the cofactor extracted from the enzyme QM/MM profile.

This trend in charge evolution of the hydride and the carbon acceptor atom is not observed in the gas phase. This means that the environment polarizes the wave function of substrate and cofactor and, as a result, electrostatic forces appear, pushing the hydride to the acceptor carbon atom in the TS. Moreover, the different shapes of the aqueous and enzymatic curves, where the slopes of the latter are smaller, suggest that the protein environment provokes the favorable electrostatic effect in a much more advanced stage of the reaction, while the water molecules effect is just in the vicinity of the TS.

Although not displayed in Figure 3, the charge on the amine group (N9, H91, and H92 as labeled in Scheme 3) and on C7 does not significantly change from reactants to products. In contrast, the charge on O8 evolves from −0.43 au in reactants to −0.55 au in products. Interestingly, the value reached in TS is, again, much closer to products than to reactants. It means that the electrostatic interaction with His332 is stronger in TS than in reactants (as previously deduced from geometry analysis), thus better polarizing the carbonyl group and, by extension, the electron charge flow from C4 to the amide group. As discussed in the previous subsection, increase in the positive charge on the C4 hydride acceptor carbon atom is related to the deformation of the amide group imposed by the enzyme. Analysis of the evolution of AM1 gas-phase Mulliken population as a function of the O8−C7−C3−C4 dihedral angle shows that charge on the C4 atom of the trans conformer (defined by the relative orientation of this dihedral angle) is 0.006 au, while the cis conformer gives a slighter more positive one (0.035 au). So, it seems that the enzyme forces the geometry of the cofactor into a geometry favorable for the reaction to occur from the electrostatic point of view, instead of minimizing it into the most stable conformation. This effect has been interpreted as an NAC effect.[70,71] These changes are in agreement with the generation of a dipolar form of the nicotinamide ring in the TS, close to the one depicted in Scheme 2,[28] which would favor the hydride transfer. Obviously, the fact that a more dramatic effect was observed in the enzyme environment (higher positive charge on C4 at TS) must be due to specific interactions with aminoacids of the protein backbone.

In the second step of the electrostatic effects study, the electric field and electrostatic potential created by the environment on the hydride position along the reaction profile has been computed. In particular, the projection of the electric field created by the protein or the aqueous solvent on the vector defined by the acceptor−donor carbon atoms, $C4_{nic}-C_{formiate}$, is displayed as a function of the position of the hydride along the reaction profile in Figure 4.

The first conclusion that can be derived from Figure 4 is that the electric field created by the protein is more robust and invariant than the one created by the water molecules, which changes significantly from reactants to products from positive

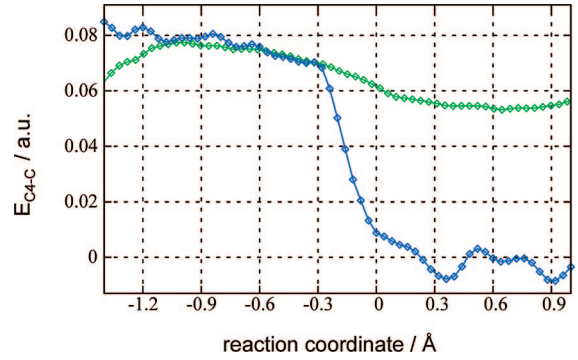

Figure 4. Evolution of the averaged projection of the electric field created by the environment, water (blue line) and enzyme (green line), on the C4−C vector as a function of the transferring hydride position.

to negative values. In fact, the projection of the electric field created by water molecules is negligible at the surroundings of the TS. Combining the information rendered by this figure with the charge evolution on the transferring hydride (Figure 3c), and remembering the classical electrostatic equation,

$$\vec{F} = q \times \vec{E} \tag{6}$$

an electrostatic force is created by the protein environment on the H_t at the TS favoring the movement of the hydride from the carbon atom of the substrate, $C_{formiate}$, to the acceptor carbon atom of the cofactor, C4. On the other side, in aqueous solution, a strong electrostatic field acts against the hydride transfer in reactants. This is so because the solvent stabilizes the charge separation existing in the solvated reactants. We must keep in mind that the reaction proceeds from charged species in reactants to neutral species in products. Thus, the solvent reaction field clearly acts against the advance of the reaction. When the system arrives to the product state, the projection of the field is negative and, keeping in mind the charge on the hydride at this state (positive), the electric field would slightly stabilize products. The products are neutral, and, consequently, the projection of the reaction electric field created by water molecules is less intense than that for the charged reactants. Thus, the enzyme is able to provide an adequate electrostatic environment for the changes taking place in the chemical system. The presence of the protein structure avoids the response of the environment as a mere consequence of the changes produced in the reaction. In this case, where the polarity of the system diminishes as the TS is reached, such a response would mean an increase of the activation energy barrier because the electrostatic interactions are weakened, as observed in aqueous solution. Note that, in this discussion, we are referring to a particular component of the electric field. In conclusion, while the aqueous solution

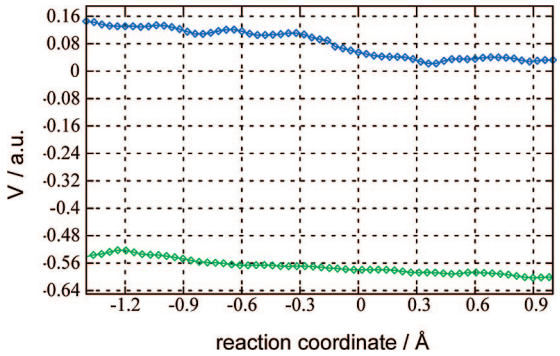

Figure 5. Evolution of the averaged electrostatic potential created by the environment, water (blue line) and enzyme (green line), as a function of the transferring hydride position.

clearly favors the stabilization of the reactant state, the protein, despite stabilizing reactants, stabilizes TS much better the than water does.

These findings are similar to the conclusions reached by Olsson and Warshel[72] and us on the analysis of the solute solvent dynamics in the S_N2 reaction of catechol methyl transferase[73] or haloalkane dehalogenase[74] compared to solution.

Finally, another comparative analysis of the electrostatic behavior of the enzyme and aqueous solution can be carried out by evaluation of the averaged electrostatic potential at positions along the vector connecting the donor and the acceptor atoms. Figure 5 is a plot of the electrostatic potential evolution on the H_t atom along the reaction coordinate for both environments. Clearly the electrostatic potential of the environment is a hindrance to the transfer of a hydride from a formate ion to the positively charged NAD^+ in water. As observed in the figure, the values are always positive in water and negative in the enzyme. In this simple model (neglecting interactions between QM atoms), the work required for hydride transfer is the product of the partial charge δq multiplied by the electrostatic potential difference ΔV.

$$W = \delta q \times \Delta V \tag{7}$$

As previously done, we have to combine this information with the charge evolution of the hydride along the reaction profile (Figure 3c). The electrostatic potential difference between reactants and the TS is smaller in the enzyme active site than in water ($\Delta V = 0.04$ and 0.08 au, respectively). Thus, although an electrostatic work is required to transfer the hydride from reactants to TS, this is smaller in the enzyme than in solution; the electrostatic potential created by the enzyme is mainly due to a permanent charge distribution, and it remains essentially unaltered as the reaction proceeds. In contrast, the reaction field in water reflects the polarization of the solvent induced by the change in the solute polarity.

Kinetic Isotope Effects. As explained in the Computational Details section, 10 selected structures from a long QM/MM MD simulation at the maximum of the PMF were refined as first-order saddle points for the hydride transfer reaction. Next, IRC paths were traced down to reactants (MC) in order to calculate effects on reaction rates arising from isotopic substitutions at different positions. The results, with correction of tunneling effects by the semiclassical Bell's equation, are listed in Table 2. The first conclusion we can derive from the analysis of the results is the small deviation observed from the 10 differently located TS structures. Single molecular studies on some enzyme mechanisms[75–80] have demonstrated that an enzymatic reaction is a stochastic event, and a single-molecule experiment measures the waiting times for the completion of the enzymatic reaction. Multiexponentiality in the probability density of these waiting times is a manifestation of dynamic disorder, that is, fluctuations with time of the catalytic rate constant of a single enzyme molecule, caused by slow transitions among different conformational substrates (reactant valleys) of the enzyme having different characteristic values of the rate constant. These fluctuations can occur on a time scale comparable to or longer than that of the enzymatic reaction. The slow interconversion among conformers results in the memory effect associated with the correlations between successive enzymatic turnover times. The overall rate of product formation is no longer governed by a single rate constant, but effectively by a distribution of rate constants. Nevertheless, it seems that KIEs, expressed as a ratio of rate constants, are less sensitive than other magnitudes as the free energy barriers.[62] A comparison of our calculated primary deuterium and secondary ^{15}N KIEs with experimental data reported in the literature for FDH catalyzed reaction reveals a very good agreement.[10,28] Thus, the results provide additional support for the conclusion that hydride-transfer is the sole rate-limiting step in *Pseudomonas* sp. FDH and the fact that N1 center of nicotinamide ring remains almost planar during the transfer (as can be deduced from the geometrical analysis of the C5−C6−C2−N1 dihedral angle reported in Table 1). Moreover, in an attempt to test the effect of His332 in polarizing the carbonyl bond of the amide moiety, secondary ^{18}O KIE on the O8 position was also computed. A small normal KIE effect of 1.0021 reveals a tighter structure in reactants than in the TS, thus suggesting a change in the bond of the amide group from double to a bond order between 2 and 1, or, in other words, a trend in the change in the O8 hybridization from sp2 to sp3. It is important to point out that this KIE-predicted value, although small, is measurable, which could encourage experimentalists to measure it. This behavior is different from the one observed on the two O atoms of formiate, which are both going from a tighter structure in reactants (sp3-like) than in TS (sp2-like), as shown in Table 2. Obviously, because of the interactions with several residues of the active site (see Scheme 3), the two oxygen atoms of formiate are not equivalent, and, in fact, data reported in Table 2 is the average of both formiate oxygen atoms.

Conclusions

Theoretical estimation of the FDH activity has been done through a combination of two hybrid QM/MM techniques: statistical simulation methods and internal energy minimizations. The reaction catalyzed by FDH, the oxidation of formate anion to carbon dioxide, has been carried out in the active site of the enzyme and in a box of water molecules to get a reference reaction for comparative purposes.

The first conclusion derived from the results is that the free energy barrier of the reaction in the enzyme, 12.4 kcal·mol^{-1}, is much smaller than the corresponding one in solution, 21.3 kcal·mol^{-1}, demonstrating the catalytic activity of the enzyme; $\Delta\Delta G^{\ddagger} = 8.9$ kcal·mol^{-1}. As these profiles do not include the work required to bring the two reactants together in an appropriate orientation, these results suggest the significant catalytic role of the enzyme in stabilizing the TS of the chemical reaction. Moreover, it must be keep in mind that the MC-like state defined in aqueous solution is not a minimum, so the 8.9 difference has to be considered as a lower limit of the free energy barrier difference between the two media. The analysis of the relative interaction energy term of the averaged MC, the MC-like in solution and TSs structures obtained from the QM/

TABLE 2: Kinetic Effects Arising from Isotopic Substitutions at Transferred Hydride, $k(^1H)/k(^2H)$, N1 Nitrogen Atom, $k(^{14}N)/k(^{15}N)$, and O Atoms of Formiate and the O Atom of the Nicotinamide Ring, $k(^{16}O)/k(^{18}O)$, Obtained at 300 K[a]

	$k(^1H)/k(^2H)$	$k(^{14}N)/k(^{15}N)$	$k(^{16}O)/k(^{18}O)_{form}$	$k(^{16}O8)/k(^{18}O8)$
1	2.7135	1.0041	0.9938	1.0016
2	2.7301	1.0041	0.9976	1.0058
3	2.7111	1.0041	1.0104	1.0019
4	2.6944	1.0041	0.9930	1.0014
5	2.7324	1.0041	0.9944	1.0017
6	2.7131	1.0040	0.9942	1.0015
7	2.7374	1.0041	0.9948	1.0018
8	2.7025	1.0040	0.9943	1.0017
9	2.7010	1.0041	0.9948	1.0018
10	2.6928	1.0041	0.9939	1.0016
average	2.713 ± 0.010	1.0041 ± 0.00003	0.996 ± 0.003	1.0021 ± 0.0008
experimental	2.8[b]	1.004 ± 0.001[c]	not measured	not measured

[a] Results are reported for 10 different structures (see text for details) and their arithmetic average. [b] From ref 10. [c] From ref 28.

MM MD simulations reveals that the catalytic character of the enzyme comes from the relative favorable enzyme−substrate interaction energy term. Solvent environment behaves as a reaction field responding the chemical changes of the substrate.

The protein restrains the ground-state of the substrate in a conformation favorable to react, by means of a series of hydrogen bond interactions with the aminoacids of the active site. In particular, analysis of the evolution of hydrogen bond interactions between formate ion and Arg284, Ile122, Asn146, and His332 along the reaction profile demonstrates, first, the important role of the enzyme by anchoring the formate ion in the MC, which also prevents side-reactions between formate and NAD^+, and, second, the stabilization of TS, in particular through interactions established between substrate and Ile122, Asn146, Arg284, or His332, and between cofactor and Thr282, Asp308, Ser334, and the binary His332−Gln313.

The observed deformation of the cofactor imposed by the protein and the relative movements of the residues are related to important electrostatic effects. This analysis has been carried out in two steps: first, by analyzing the charge evolution on the key atoms of substrate and cofactor under the effect of the aqueous solution or by the protein, and, second, by more global effects, which are the electric field and the electrostatic potential created by the environment on the hydride position along the reaction. The calculations show how the charge evolution on the C4 atom, the acceptor atom, reaches a maximum in the TS, while the charge on the transferring hydride in the TS is an absolute minimum; this evolution is not observed in the gas phase. This means that the environment polarizes the wave function of substrate and cofactor, and an electrostatic force appears to push the hydride to the acceptor carbon atom in the TS. These changes are in agreement with the generation of a dipolar form of nicotinamide ring in the TS, which would favor the hydride transfer. The enzyme environment would create a more positively charged acceptor C4 atom than aqueous environment as a result of specific interactions with aminoacids of the protein backbone, thus explaining, to some extent, the catalytic effect.

The conclusion that can be derived from the analysis of the electric field created by the protein is that it seems to be more robust and invariant than the one created by the water molecules, which changes significantly from reactants to products. In fact, the projection of the electric field created by water solvent is negligible at the surroundings of the TS. Combining this information with the charge evolution on the transferring hydride, an electrostatic force is created by the protein environment on the Ht at the TS, favoring the movement of the hydride from the carbon atom of the substrate to the acceptor carbon atom of the cofactor. Thus, it seems that the enzyme is creating a favorable local electric field on the vector defined by the donor and acceptor carbon atoms to favor the hydride transfer. On the other side, in aqueous solution, a strong electrostatic field is acting against the hydride transfer in reactants. This is so because the solvent stabilizes the charge separation existing in the solvated reactants. The presence of the protein structure avoids the response of the environment as a mere consequence of the changes produced in the reaction. In this case, where the polarity of the system diminishes as the TS is reached, such a response would mean an increase in the activation energy barrier because the electrostatic interactions are weakened, as observed in aqueous solution. In conclusion, while the aqueous solution clearly favors the stabilization of the reactant state, the protein, albeit stabilizing reactants, stabilizes much better the TS than does water.

The averaged electrostatic potential at positions along the vector connecting the donor and the acceptor atoms shows that, although an electrostatic work is required to transfer the hydride from reactants to TS, this is smaller in the enzyme than in solution; the electrostatic potential created by the enzyme is mainly due to a permanent charge distribution, and thus it remains essentially unaltered as the reaction proceeds. In contrast, the reaction field in water reflects the polarization of the solvent induced by the change in the solute polarity.

Finally, a comparison of our calculated primary deuterium and secondary ^{15}N KIEs with experimental data reported in the literature for FDH-catalyzed reactions reveals a very good agreement. Thus, the results provide additional support for the conclusion that hydride-transfer is the sole rate-limiting step in *Pseudomonas* sp. FDH and the fact that the N1 center of nicotinamide ring remains almost planar during the transfer. Moreover, in an attempt to test the effect of His332 in polarizing the carbonyl bond of the amide moiety, secondary ^{18}O KIE on the O8 position reveals a tighter structure in reactants than in the TS, thus suggesting a change in the bond of the amide group that facilitates the reaction. These predicted KIE values, although small, are measurable, which could encourage experimentalists to measure it.

Acknowledgment. This work was supported by DGI project CTQ2006-15447-C02-01/BQU, BANCAIXA projects P1•1B2005-13 and P1•1B2005-27, and Generalitat Valenciana projects GV06/152 and GV06/016. We acknowledge the Servei d'Informàtica of the Universitat Jaume I for providing us with computer capabilities.

Supporting Information Available: Free energy profile obtained by means of the FEP method for oxidation of formate anion to carbon dioxide in aqueous solution. This material is available free of charge via the Internet at http://pubs.acs.org.

References and Notes

(1) Tishkov, V. I.; Popov, V. O. *Biomol. Eng.* **2006**, *23*, 89.
(2) Wichmann, R.; Wandrey, C.; Buckmann, A. F.; Kula, M. R. *Biotechnol. Bioeng.* **2000**, *67*, 791.
(3) Krix, G.; Bommarius, A. S.; Drauz, K.; Kottenhahn, M.; Schwarm, M.; Kula, M. R. *J. Biotechnol.* **1997**, *53*, 29.
(4) Tishkov, V. I.; Popov, V. O. *Biochemistry (Moscow)* **2004**, *69*, 1252.
(5) Mesentsev, A. V.; Lamzin, V. S.; Tishkov, V. I.; Ustinnikova, T. B.; Popov, V. O. *Biochem. J.* **1997**, *321*, 475.
(6) Schaller, K. H.; Triebig, G. In *Methods in Enzymatic Analysis*; Bergmeyer, H. U., Ed.; VCH: Weinheim, Germany, 1994; Vol. 6; p 668.
(7) Hatch, M.; Bourke, E.; Costello, J. *Clin. Chem.* **1977**, *23*, 76.
(8) Rojkova, A. M.; Galkin, A. G.; Kulakova, L. B.; Serov, A. E.; Savitsky, P. A.; Fedorchuk, V. V.; Tishkov, V. I. *FEBS Lett.* **1999**, *445*, 183.
(9) Xue, H.; Wu, X. W.; Huskey, W. P. *J. Am. Chem. Soc.* **1996**, *118*, 5804.
(10) Blanchard, J. S.; Cleland, W. W. *Biochemistry* **1980**, *19*, 3543.
(11) Hermes, J. D.; Morrical, S. W.; O′Leary, M. H.; Cleland, W. W. *Biochemistry* **1984**, *23*, 5479.
(12) Tishkov, V. I.; Galkin, A. G.; Yegorov, A. M. *Dokl. Akad. Nauk SSSR* **1991**, *317*, 745.
(13) Iida, M.; Kitamura-Kimura, K.; Maeda, H.; Mineki, S. *Biosci. Biotechnol. Biochem.* **1992**, *56*, 1966.
(14) Schiøtt, B.; Zheng, Y. J.; Bruice, T. C. *J. Am. Chem. Soc.* **1998**, *120*, 7192.
(15) Lamzin, V. S.; Dauter, Z.; Popov, V. O.; Harutyunyan, E. H.; Wilson, K. S. *J. Mol. Biol.* **1994**, *236*, 759.
(16) Li, H.; Goldstein, B. M. *J. Med. Chem.* **1992**, *35*, 3560.
(17) Popov, V. O.; Lamzin, V. S. *Biochem. J.* **1994**, *301*, 625.
(18) Wu, Y. D.; Houk, K. N. *J. Am. Chem. Soc.* **1987**, *109*, 2226.
(19) Wu, Y. D.; Houk, K. N. *J. Am. Chem. Soc.* **1987**, *109*, 906.
(20) Wu, Y. D.; Houk, K. N. *J. Am. Chem. Soc.* **1991**, *113*, 2353.
(21) Wu, Y. D.; Houk, K. N. *J. Org. Chem.* **1993**, *58*, 2043.
(22) Wu, Y. D.; Lai, D. K. W.; Houk, K. N. *J. Am. Chem. Soc.* **1995**, *117*, 4100.
(23) Almarsson, Ö.; Bruice, T. C. *J. Am. Chem. Soc.* **1993**, *115*, 2125.
(24) Almarsson, Ö.; Karaman, R.; Bruice, T. C. *J. Am. Chem. Soc.* **1992**, *114*, 8702.
(25) Olson, L. P.; Bruice, T. C. *Biochemistry* **1995**, *34*, 7335.
(26) Olson, L. P.; Luo, J.; Almarsson, O.; Bruice, T. C. *Biochemistry* **1996**, *35*, 9782.
(27) Tapia, O.; Andrés, J.; Cardenas, R. *Chem. Phys. Lett.* **1992**, *189*, 395.
(28) Rotberg, N. S.; Cleland, W. W. *Biochemistry* **1991**, *30*, 4068.
(29) Mestres, J.; Durán, M.; Bertran, J. *Bioorg. Chem.* **1996**, *24*, 69.
(30) Cunningham, M. A.; Ho, L. L.; Nguyen, D. T.; Gillilan, R. E.; Bash, P. A. *Biochemistry* **1997**, *36*, 4800.
(31) Cummins, P. L.; Gready, J. E. *J. Comput. Chem.* **1990**, *11*, 791.
(32) Buck, H. M. *Recl. Trav. Chim. Pays−Bas* **1996**, *115*, 329.
(33) Andrés, J.; Moliner, V.; Safont, V. S. *J. Phys. Org. Chem.* **1996**, *9*, 498.
(34) Andrés, J.; Moliner, V.; Safont, V. S.; Domingo, L. R.; Picher, M. T. *J. Org. Chem.* **1996**, *61*, 7777.
(35) Andrés, J.; Moliner, V.; Safont, V. S.; Domingo, L. R.; Picher, M. T.; Krechl, J. *Bioorg. Chem.* **1996**, *24*, 10.
(36) LaReau, R. D.; Wan, W.; Anderson, V. E. *Biochemistry* **1989**, *28*, 3619.
(37) Tishkov, V. I.; Matorin, A. D.; Rojkova, A. M.; Fedorchuk, V. V.; Savitsky, P. A.; Dementieva, L. A.; Lamzin, V. S.; Mezentzev, A. V.; Popov, V. O. *FEBS Lett.* **1996**, *390*, 104.
(38) Galkin, A. G.; Kutsenko, A. S.; Bajulina, N. P.; Esipova, N. G.; Lamzin, V. S.; Mesentsev, A. V.; Shelukho, D. V.; Tikhonova, T. V.; Tishkov, V. I.; Ustinnikova, T. B.; Popov, V. O. *Biochim. Biophys. Acta* **2002**, *1594*, 136.
(39) Clarke, A. R.; Wigley, D. B.; Chia, W. N.; Barstow, D.; Atkinson, T.; Holbrook, J. J. *Nature* **1986**, *324*, 699.
(40) Torres, R. A.; Schiøtt, B.; Bruice, T. C. *J. Am. Chem. Soc.* **1999**, *121*, 8164.
(41) In ref 40, Bruice et al. located the TS by gas-phase *ab initio* calculations and placed it afterwards into the cavity of the enzyme at frozen geometry by high force constants for the bond lengths and angles, essentially making it a rigid body treated classically.
(42) Field, M. J. *A Practical Introduction to the Simulation of Molecular Systems*; Cambridge University Press: Cambridge, U.K., 1999.
(43) Field, M. J.; Albe, M.; Bret, C.; Proust-De Martin, F.; Thomas, A. *J. Comput. Chem.* **2000**, *21*, 1088.
(44) Dewar, M. J. S.; Zoebisch, E. G.; Healy, E. F.; Stewart, J. J. P. *J. Am. Chem. Soc.* **1985**, *107*, 3902.
(45) Kaminski, G. A.; Friesner, R. A.; Tirado-Rives, J.; Jorgensen, W. L. *J. Phys. Chem. B* **2001**, *105*, 6474.
(46) Jorgensen, W. L.; Chandrasekhar, J.; Madura, J. D.; Impey, R. W.; Klein, M. L. *J. Chem. Phys.* **1983**, *79*, 926.
(47) Field, M. J.; Bash, P. A.; Karplus, M. *J. Comput. Chem.* **1990**, *11*, 700.
(48) Warshel, A.; Levitt, M. *J. Mol. Biol.* **1976**, *103*, 227.
(49) Martí, S.; Moliner, V.; Tuñón, I. *J. Chem. Theory Comput.* **2005**, *1*, 1008.
(50) Kumar, S.; Bouzida, D.; Swendsen, R. H.; Kollman, P. A.; Rosenberg, J. M. *J. Comput. Chem.* **1992**, *13*, 1011.
(51) Torrie, G. M.; Valleau, J. P. *J. Comput. Phys.* **1977**, *23*, 187.
(52) Melissas, V. S.; Truhlar, D. G.; Garrett, B. C. *J. Chem. Phys.* **1992**, *96*, 5758.
(53) Williams, I. H. *THEOCHEM (J. Mol. Struct.)* **1983**, *11*, 275.
(54) Williams, I. H. *Chem. Phys. Lett.* **1982**, *88*, 462.
(55) Sühnel, J.; Schowen, R. L. *Enzyme Mechanism from Isotope Effects*; CRC Press: Boca Raton, FL, 1991.
(56) Bell, R. P. *Trans. Faraday Soc.* **1959**, *55*, 1.
(57) Breneman, C. M.; Wiberg, K. B. *J. Comput. Chem.* **1990**, *11*, 361.
(58) Anglada, J. M.; Bofill, J. M. *J. Comput. Chem.* **1998**, *19*, 349.
(59) For a discussion about the origin of enzyme catalysis and, in particular, tunneling contribution to rate enhancement in enzyme catalysis, see Borman, S. *Chem. & Eng. News.* **2004** (Feb. 23), 35.
(60) Martí, S.; Andrés, J.; Moliner, V.; Silla, E.; Tuñón, I.; Bertran, J.; Field, M. J. *J. Am. Chem. Soc.* **2001**, *123*, 1709.
(61) Ferrer, S.; Silla, E.; Tuñón, I.; Oliva, M.; Moliner, V.; Williams, I. H. *Chem. Commun.* **2005**, 5873.
(62) Ferrer, S.; Tuñón, I.; Martí, S.; Moliner, V.; Garcia-Viloca, M.; Gonzalez-Lafont, A.; Lluch, J. M. *J. Am. Chem. Soc.* **2006**, *128*, 16851.
(63) Moliner, V.; Williams, I. H. *Chem. Commun.* **2000**, 1843.
(64) Shinoda, T.; Arai, K.; Shigematsu-Iida, M.; Ishikura, Y.; Tanaka, S.; Yamada, T.; Kimber, M. S.; Pai, E. F.; Fushinobu, S.; Taguchi, H. *J. Biol. Chem.* **2005**, *280*, 17068.
(65) Kochhar, S.; Hunziker, P. E.; Leong-Morgenthaler, P.; Hottinger, H. *J. Biol. Chem.* **1992**, *267*, 8499.
(66) Bernard, N.; Ferain, T.; Garmyn, D.; Hols, P.; Delcour, J. *FEBS Lett.* **1991**, *290*, 61.
(67) Taguchi, H.; Ohta, T. *J. Biol. Chem.* **1991**, *266*, 12588.
(68) Holbrook, J. J.; Liljas, A.; Steindel, S. J.; Rossmann, M. G. In *The Enzymes*, 3rd ed.; Boyer, P. D., Ed.; Academic Press: New York, 1975; Vol. 11, p 191.
(69) Bandaria, J. N.; Dutta, S.; Hill, S. E.; Kohen, A.; Cheatum, C. M. *J. Am. Chem. Soc.* **2008**, *130*, 22.
(70) Lightstone, F. C.; Bruice, T. C. *J. Am. Chem. Soc.* **1996**, *118*, 2595.
(71) Lightstone, F. C.; Bruice, T. C. *J. Am. Chem. Soc.* **1997**, *119*, 9103.
(72) Olsson, M. H. M.; Warshel, A. *J. Am. Chem. Soc.* **2004**, *126*, 15167.
(73) Roca, M.; Andrés, J.; Moliner, V.; Tuñón, I.; Bertran, J. *J. Am. Chem. Soc.* **2005**, *127*, 10648.
(74) Soriano, A.; Silla, E.; Tuñón, I.; Ruiz-Lopez, M. F. *J. Am. Chem. Soc.* **2005**, *127*, 1946.
(75) Min, W.; English, B. P.; Luo, G. B.; Cherayil, B. J.; Kou, S. C.; Xie, X. S. *Acc. Chem. Res.* **2005**, *38*, 923.
(76) Antikainen, N. M.; Smiley, R. D.; Benkovic, S. J.; Hammes, G. G. *Biochemistry* **2005**, *44*, 16835.
(77) Kou, S. C.; Cherayil, B. J.; Min, W.; English, B. P.; Xie, X. S. *J. Phys. Chem. B* **2005**, *109*, 19068.
(78) Smiley, R. D.; Hammes, G. G. *Chem. Rev.* **2006**, *106*, 3080.
(79) Lu, H. P.; Xun, L. Y.; Xie, X. S. *Science* **1998**, *282*, 1877.
(80) Yang, H.; Luo, G. B.; Karnchanaphanurach, P.; Louie, T. M.; Rech, I.; Cova, S.; Xun, L. Y.; Xie, X. S. *Science* **2003**, *302*, 262.

JP8025896